

# Mono- and Di-chloro-bridged Discrete Dimers and Trimers and Mono-Chloro-Bridged 1D-Coordination Polymer of Copper(II). Magneto-structural Studies

Ravindra Singh,<sup>[a]</sup> Francesc Lloret,<sup>[b]</sup> and Rabindranath Mukherjee\*<sup>[a,c]</sup>

*Dedicated to Professor C. N. R. Rao on the Occasion of His 80th Birthday*

**Keywords:** Mono-chloro-bridges; Copper(II) complexes; Discrete trimer and 1D polymeric chain; Cu<sub>2</sub>Cl<sub>2</sub> dimer; Crystal structures; Magnetic properties

**Abstract.** The synthesis, structural characterization, and magnetic properties of three copper(II) complexes, a mono-chloro-bridged [Cu<sup>II</sup>(L<sup>6</sup>)<sub>2</sub>(μ-Cl)(Cl)(Cu<sup>II</sup>Cl<sub>4</sub>)] (1) and a dichloro-bridged [Cu<sup>II</sup><sub>2</sub>(L<sup>7</sup>)<sub>2</sub>(μ-Cl)<sub>2</sub>][ClO<sub>4</sub>]<sub>2</sub> (3) discrete trimers and dimers, and a mono-chloro-bridged 1D-coordination polymer [Cu<sup>II</sup>(L<sup>6</sup>)(μ-Cl)][ClO<sub>4</sub>·CH<sub>3</sub>CN] (2), are reported. Molecular structures were authenticated by X-ray crystallography. Temperature-dependent magnetic measurements carried out on powdered samples of 1–3 indicated a very weak antiferromagnetic exchange-coupling within the {Cu<sup>II</sup>(μ-Cl)Cu<sup>II</sup>(μ-Cl)Cu<sup>II</sup>Cl<sub>3</sub>}<sup>+</sup> units in

1 [Curie-Weiss plot:  $\theta = -0.19(1)$  K and  $g = 2.07(1)$ ], a ferromagnetic behavior within {Cu<sup>II</sup>(μ-Cl)<sub>2</sub>Cu<sup>II</sup>}<sup>2+</sup> units in 3 [ $\hat{H} = -JS_1 \cdot S_2$ :  $J = +6.0(1)$  cm<sup>-1</sup>,  $D$  (zero-field splitting parameter) =  $4.5(2)$  cm<sup>-1</sup>, and  $g = 2.11$ ], and a weak intrachain antiferromagnetic behavior due to {Cu<sup>II</sup>(μ-Cl)Cu<sup>II</sup>}<sup>3+</sup> units in 2 [single-chain polymer:  $J = -0.20(1)$  cm<sup>-1</sup> and  $g = 2.11$ ]. The square-pyramidal stereochemistry of the central copper(II) atoms in 1–3 was identified by their absorption spectral properties in acetonitrile. An attempt was made to rationalize the observed magneto-structural behavior.

## Introduction

The magnetic properties of transition metal complexes are of great importance both from the point of view of basic research and also because of their potential applications.<sup>[1–3]</sup> From this perspective the magnetic studies of dinuclear discrete complexes containing paramagnetic centers connected through various types of bridges (e.g. oxo, hydroxo, alkoxo, phenoxo, acetato, azido, chloro, pyrazolato etc.)<sup>[4–20]</sup> continue to attract widespread attention. Investigation and understanding of the nature and extent of magnetic-exchange coupling between the paramagnetic centers from the standpoint of magneto-structural aspects are very important for designing new molecular magnetic materials.<sup>[21]</sup> Emphasis is always directed to look for meaningful correlations between the structural and

magnetic properties, expressed as exchange coupling constant  $J$  (ferromagnetic coupling:  $J > 0$ ; antiferromagnetic coupling:  $J < 0$ ). The study of magnetic interaction between the central metal atoms in dinuclear ligand-bridged copper(II) complexes remains the center of magneto-structural investigations.

This report is concerned with both discrete and coordination polymeric mono-<sup>[18]</sup> and discrete di-chloro-bridged<sup>[14,16,18i,19]</sup> copper(II) complexes. The magnitude of the coupling between magnetic orbitals of two central copper(II) atoms in singly chloro-bridged systems is mainly related to the Cu–Cl–Cu bridge angle, Cu–Cl distance, and nature of the terminal ligand.<sup>[18]</sup> For doubly chloro-bridged square-pyramidal dimeric copper(II) complexes, Hatfield<sup>[16]</sup> provided a correlation between the  $J$  (singlet-triplet energy gap) and the structural parameter  $\phi/R$  in deg·Å<sup>-1</sup>, where  $\phi$  is the bridging Cu–Cl–Cu angle and  $R$  is the long Cu–Cl bond length. Antiferromagnetic coupling is observed for values of  $\phi/R$  below 32.6 or above 34.8, while ferromagnetic exchange is found for the values of  $\phi/R$  between these limits.

Using two tridentate N-donor ligands L<sup>1</sup> and L<sup>2</sup> we reported<sup>[22a]</sup> structural properties of two discrete dimeric Cu<sup>II</sup>(μ-Cl)<sub>2</sub>Cu<sup>II</sup> complexes [{(L<sup>1</sup>)Cu<sup>II</sup>(μ-Cl)(OCIO<sub>3</sub>)<sub>2</sub>}]<sub>2</sub> and [{(L<sup>2</sup>)Cu<sup>II</sup>(μ-Cl)(OCIO<sub>3</sub>)<sub>2</sub>}]<sub>2</sub>. Using a *m*-xylyl-based dinucleating ligand L<sup>3</sup> we reported<sup>[22b]</sup> a complex of composition “Cu<sup>II</sup>(L<sup>3</sup>)Cl<sub>2</sub>”; magneto-structural studies revealed it to be a 3D-coordination polymer with {Cu<sup>II</sup>(μ-Cl)<sub>2</sub>Cu<sup>II</sup>}<sup>2+</sup> repeating units and the central copper(II) atoms are antiferromagnetically coupled ( $J = -10$  cm<sup>-1</sup>). We extended our investigation with

\* Prof. Dr. R. Mukherjee  
Fax: +91 512 2597437

E-Mail: rnm@iitk.ac.in

[a] Department of Chemistry  
Indian Institute of Technology Kanpur  
Kanpur 208 016, India

[b] Departament de Química  
Inorgànica/Instituto de Ciencia Molecular (ICMOL)  
Universitat de València, Polígono de la Coma, s/n  
46980-Paterna (València), Spain

[c] Present address:  
Indian Institute of Science Education and Research Kolkata  
Mohanpur Campus  
Mohanpur 741 252, India

Supporting information for this article is available on the WWW under <http://dx.doi.org/10.1002/zaac.201400005> or from the author.

the use of two more *m*-xylyl-based ligands  $L^4$  and  $L^5$  and reported<sup>[22c]</sup> magneto-structural studies of 1D-coordination polymeric complexes  $[\text{Cu}^{\text{II}}_2(\text{L}^4)\text{Cl}_2][\text{ClO}_4]_2 \cdot \text{CH}_3\text{CN} \cdot \text{THF}$  and  $[\text{Cu}^{\text{II}}_2(\text{L}^5)\text{Cl}_2][\text{ClO}_4]_2 \cdot \text{CH}_3\text{CN}$ , respectively. In discrete dimeric and 1D coordination polymeric complexes of  $L^1/L^2$  and  $L^4/L^5$ , respectively, each central  $\text{Cu}^{\text{II}}$  atom assumes square-pyramidal arrangement, encompassing base-to-apex edge-sharing with parallel basal planes. The magnetic properties of  $[(\text{L}^2)\text{Cu}^{\text{II}}(\mu\text{-Cl})(\text{ClO}_4)]_2$ ,  $[\text{Cu}^{\text{II}}_2(\text{L}^4)\text{Cl}_2][\text{ClO}_4]_2 \cdot \text{CH}_3\text{CN} \cdot \text{THF}$ , and  $[\text{Cu}^{\text{II}}_2(\text{L}^5)\text{Cl}_2][\text{ClO}_4]_2 \cdot \text{CH}_3\text{CN}$  revealed the presence of weakly antiferromagnetic  $J = -3.89 \text{ cm}^{-1}$  and  $-1.84 \text{ cm}^{-1}$ , and ferromagnetic  $J = +6.27 \text{ cm}^{-1}$ , respectively.<sup>[22c]</sup> The ligands of pertinence of this investigation are in Figure 1.

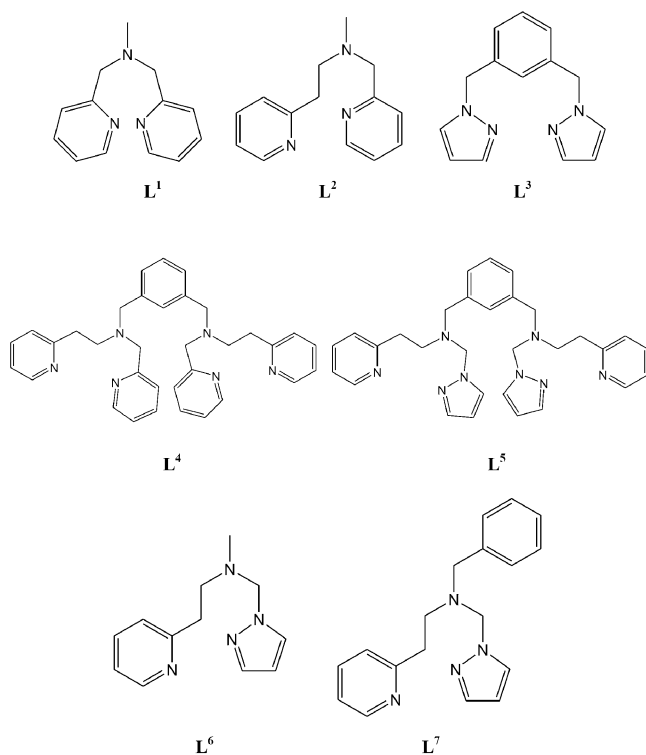


**Figure 1.** Ligands of pertinence to this work.

In this work, we have considered two new tridentate N-donor ligands  $L^6$  and  $L^7$  to synthesize chloro-bridged complexes  $[\text{Cu}_2^{\text{II}}(\text{L}^6)_2(\mu\text{-Cl})(\text{Cl})(\text{Cu}^{\text{II}}\text{Cl}_4)]$  (**1**) and  $[\text{Cu}_2^{\text{II}}(\text{L}^7)_2(\mu\text{-Cl})_2][\text{ClO}_4]_2$  (**3**), and 1D coordination polymer  $[\text{Cu}^{\text{II}}(\text{L}^6)(\mu\text{-Cl})][\text{ClO}_4] \cdot \text{CH}_3\text{CN}$  (**2**). The structures of all the three complexes were elucidated by single-crystal X-ray crystallography. The magnetic properties of **1–3** were analyzed and the observed results compared with similar kind of complexes reported in the literature.

## Experimental Section

**Materials and Reagents:** All reagents were obtained from commercial sources and used without further purification, unless otherwise stated. Pyrazole-1-carbinol was prepared as reported in the literature.<sup>[23]</sup> The ligands  $L^6$  and  $L^7$  were prepared by following a reported procedure.<sup>[10d]</sup>

**Physical Measurements:** Elemental analyses were obtained with a Thermo Quest EA 1110 CHNS-O, Italy. Spectroscopic measurements were made using the following instruments: IR (KBr, 4000–600  $\text{cm}^{-1}$ ), Bruker Vector 22. UV/Vis, Perkin-Elmer Lambda 2 and Agilent 8453 diode-array spectrophotometers.  $^1\text{H}$  NMR spectra were obtained with a JEOL JNM LA (500 MHz) spectrophotometer. Chemical shifts are reported in ppm referenced to TMS.

### *N*-{(Pyrazol-1-yl)methyl}-*N*-methyl-2-(pyridin-2-yl)ethanamine

(**L**<sup>6</sup>): *N*-methyl-2-(aminoethyl-2-pyridine) (1.01 g, 7.45 mmol) and pyrazole-1-carbinol (0.730 g, 7.45 mmol) were dissolved in dry acetonitrile (60 mL). The resulting solution was purged with nitrogen and stirred for 4 d at room temperature. The reaction mixture was dried with anhydrous  $\text{Na}_2\text{SO}_4$  and after filtration the solvent was evaporated under reduced pressure. The desired ligand was obtained as thick brownish yellow oil. Yield: 1.4 g, 87%.  $\text{C}_{12}\text{H}_{16}\text{N}_4$  ( $M_r = 216.28 \text{ g}\cdot\text{mol}^{-1}$ ): calcd. C 66.58, H 7.40, N 26.89%; found C 66.12, H 6.96, N 26.80%.  $^1\text{H}$  NMR (500 MHz,  $\text{CDCl}_3/\text{TMS}$ ):  $\delta = 2.40$  (s, 3 H,  $-\text{NCH}_3$ ), 2.91 (t, 2 H,  $-\text{CH}_2-$ ), 2.98 (t, 2 H,  $-\text{CH}_2-$ ), 4.97 (s, 2 H,  $-\text{CH}_2-$  of pyrazole), 6.26 (t, 1 H, pyrazole  $\text{H}^4$ ), 7.12 (t, 1 H, pyridine  $\text{H}^5$ ), 7.17 (d, 1 H, pyridine  $\text{H}^3$ ), 7.43 (d, 1 H, pyrazole  $\text{H}^3$ ), 7.52 (d, 1 H, pyrazole  $\text{H}^5$ ), 7.59 (t, 1 H, pyridine  $-\text{H}^4$ ), 8.51 (d, 1 H, pyridine  $\text{H}^6$ ) ppm.

### *N*-{(Pyrazol-1-yl)methyl}-*N*-benzyl-2-(pyridin-2-yl)ethanamine

(**L**<sup>7</sup>): The synthetic strategy comprises the following two steps.

***N*-Benzyl-2-(pyridin-2-yl)ethanamine:** Benzaldehyde (1.33 g, 12.59 mmol) was dissolved in dry ethanol (40 mL) and a solution of 2-(2-aminoethyl)pyridine (1.53 g, 12.59 mmol) in dry ethanol (10 mL) was added dropwise. After completion of the addition, the resulting solution was refluxed for 3 h. The solution was cooled to room temperature, the solvent was removed under reduced pressure, and the thick brown oil that obtained was dissolved in dry methanol (15 mL) and heated on a steam bath. To it excess  $\text{NaBH}_4$  (1.9 g, 50.35 mmol) was added in small portions. After each addition, the mixture was thoroughly shaken. After cooling, to the resulting mixture 25 mL of a saturated brine solution was added and the ligand was extracted with diethyl ether (50 mL). The organic layer was collected and kept with anhydrous  $\text{K}_2\text{CO}_3$ . After filtration, the solvent was evaporated under reduced pressure. The desired amine was obtained as thick yellow oil. Yield: 2.3 g, 90%.  $\text{C}_{14}\text{H}_{16}\text{N}_2$  ( $M_r = 212.29 \text{ g}\cdot\text{mol}^{-1}$ ): calcd. C 79.14, H 7.54, N 13.19%; found C 79.10, H 7.58, N 13.31%.  $^1\text{H}$  NMR (500 MHz,  $\text{CDCl}_3/\text{TMS}$ ):  $\delta = 2.05$  (s (br), 1 H,  $-\text{NH}-$ ), 3.05 (m, 4 H,  $-\text{CH}_2\text{CH}_2-$  of pyridine), 3.84 (s, 2 H,  $-\text{CH}_2-$  of benzene), 7.31–7.10 (m, 7 H, arom. proton), 7.59 (t, 1 H, pyridine  $\text{H}^4$ ), 8.53 (d, 1 H, pyridine  $\text{H}^6$ ) ppm.

***N*-{(Pyrazol-1-yl)methyl}-*N*-benzyl-2-(pyridin-2-yl)ethanamine:** *N*-Benzyl-2-(pyridin-2-yl)ethanamine (0.44 g, 2.07 mmol) and pyrazole-1-carbinol (0.098 g, 2.07 mmol) were dissolved in dry acetonitrile (25 mL). The resulting solution was purged with nitrogen and stirred for 4 d at 298 K. The solution was dried with anhydrous  $\text{Na}_2\text{SO}_4$  and after filtration the solvent was evaporated under reduced pressure. The desired ligand was obtained as thick brownish yellow oil. Yield: 0.5 g, 82%.  $\text{C}_{18}\text{H}_{20}\text{N}_4$  ( $M_r = 292.38 \text{ g}\cdot\text{mol}^{-1}$ ): calcd. C 73.88, H 6.84, N 19.15%; found C 74.12, H 6.96, N 19.24%.  $^1\text{H}$  NMR (500 MHz,  $\text{CDCl}_3/\text{TMS}$ ):  $\delta = 3.02$  (m, 4 H,  $-\text{CH}_2\text{CH}_2-$  of pyridine), 3.73 (s, 2 H,  $-\text{CH}_2-$  of benzene), 4.98 (s, 2 H,  $-\text{CH}_2-$  of pyrazole), 6.26 (s, 1 H, pyrazole  $\text{H}^4$ ), 7.58–7.09 (m, 10 H, arom. proton), 8.50 (d, 1 H, pyridine  $\text{H}^6$ ) ppm.

**$[\text{Cu}_2^{\text{II}}(\text{L}^6)_2(\mu\text{-Cl})(\text{Cl})(\text{Cu}^{\text{II}}\text{Cl}_4)]$  (**1**):** To a solution of  $L^6$  (0.048 g, 0.22 mmol) in acetonitrile (4 mL), solid  $\text{Cu}^{\text{II}}\text{Cl}_2 \cdot 2\text{H}_2\text{O}$  (0.057 g, 0.33 mmol) was added portion-wise. The color of the solution changed

from light yellow to green. The solution was stirred for 2 h at 298 K. The green solid that formed was filtered and washed with acetonitrile/diethyl ether (1:3; v/v) mixture. The resulting green solid was recrystallized by diffusion of diethyl ether into a solution of the complex in methanol and dried in vacuo. Yield: 0.055 g, 60%. Dark green single-crystals suitable for X-ray diffraction studies were obtained by slow diffusion of diethyl ether into a solution of the complex in methanol.  $C_{24}H_{32}Cl_6Cu_3N_8$  ( $M_r$ : 835.9 g·mol<sup>-1</sup>): calcd. C 34.45, H 3.83, N 13.40%; found C 34.44, H 4.16, N 13.62%. **UV/Vis** [ $\lambda_{max}$ , nm ( $\epsilon$ , M<sup>-1</sup>·cm<sup>-1</sup>)] (in methanol): 690 (320), 285 (8960), 245 (16 600).

**[Cu<sup>II</sup>(L<sup>6</sup>)( $\mu$ -Cl)] [ClO<sub>4</sub>] $\cdot$ CH<sub>3</sub>CN (2):** To a magnetically stirred solution of L<sup>6</sup> (0.050 g, 0.231 mmol) in ethanol (3 mL) was added dropwise an ethanol solution (2 mL) of Cu<sup>II</sup>Cl<sub>2</sub>·2H<sub>2</sub>O (0.04 g, 0.231 mmol). The resulting blue solution was stirred for 1 h at 298 K. Afterwards, 1 mL of a concentrated aqueous solution of NaClO<sub>4</sub>·H<sub>2</sub>O (0.130 g, 0.924 mmol) was added to it. After 15 min of stirring, the solution was filtered, and the filtrate was kept for slow evaporation. A blue solid that formed was recrystallized by diffusion of diethyl ether into a solution of the complex in acetonitrile and dried in vacuo. Yield: 0.053 g, 50%. Single-crystals suitable for X-ray diffraction were obtained by slow diffusion of diethyl ether into a solution of the complex in acetonitrile.  $C_{14}H_{19}Cl_2CuN_5O_4$  ( $M_r$  = 455.78 g·mol<sup>-1</sup>): calcd. C 36.86, H 4.17, N 15.36%; found C 37.26, H 4.96, N 15.92%. Conductivity (acetonitrile, 1 mM solution at 298 K):  $\Lambda_M$  = 130  $\Omega^{-1}$  cm<sup>2</sup> mol<sup>-1</sup> (expected range<sup>[24]</sup> for 1:1 electrolyte: 100–160  $\Omega^{-1}$  cm<sup>2</sup> mol<sup>-1</sup>). **IR** (KBr, selected peaks):  $\tilde{\nu}$  = 1116, 628 [ClO<sub>4</sub><sup>-</sup>] cm<sup>-1</sup>. **UV/Vis** [ $\lambda_{max}$ , nm ( $\epsilon$ , M<sup>-1</sup>·cm<sup>-1</sup>)] (in acetonitrile): 650 (130), 290 (3920), 260 (6500).

**[Cu<sup>II</sup><sub>2</sub>(L<sup>7</sup>)<sub>2</sub>( $\mu$ -Cl)<sub>2</sub>] [ClO<sub>4</sub>]<sub>2</sub> (3):** Cu<sup>II</sup>Cl<sub>2</sub>·2H<sub>2</sub>O (0.031 g, 0.184 mmol) was added to a solution of L<sup>7</sup> (0.054 g, 0.184 mmol) in ethanol (4 mL). Green reaction mixture thus obtained was stirred for 1 h at 298 K. Afterwards, 1 mL of a saturated aqueous solution of NaClO<sub>4</sub>·H<sub>2</sub>O (0.104 g, 0.739 mmol) was added to it. The color of the solution changed from green to blue. After 1 h of stirring, a blue compound precipitated out. It was collected by filtration and dried in vacuo. The product was recrystallized by diffusion of diethyl ether into a solution of the complex in acetonitrile. Yield: 0.058 g, 64%. Single-crystals suitable for X-ray diffraction studies were obtained by diffusion of diethyl ether into a solution of the complex in acetonitrile.  $C_{36}H_{40}Cl_4Cu_2N_6O_8$  ( $M_r$  = 981.64 g·mol<sup>-1</sup>): calcd. C 44.01, H 4.08, N 8.56%; found C 44.58, H 4.54, N 8.42%. Conductivity (acetonitrile, 1 mM solution at 298 K):  $\Lambda_M$  = 240  $\Omega^{-1}$  cm<sup>2</sup> mol<sup>-1</sup> (expected range<sup>[24]</sup> for 1:2 electrolyte: 220–300  $\Omega^{-1}$  cm<sup>2</sup> mol<sup>-1</sup>). **IR** (KBr, selected peaks):  $\tilde{\nu}$  = 1094, 622 [ClO<sub>4</sub><sup>-</sup>] cm<sup>-1</sup>. **UV/Vis** [ $\lambda_{max}$ , nm ( $\epsilon$ , M<sup>-1</sup>·cm<sup>-1</sup>)] (in acetonitrile): 660 (280), 290 (11 700), 264 (18 300).

**Caution.** Perchlorate salts are potentially explosive. Caution is advised and handling of only small quantities is recommended.

**Single Crystal Structure Analysis:** Single-crystals of suitable dimensions were used for data collection. Diffraction intensities were collected with a Bruker SMART APEX CCD diffractometer, with graphite-monochromated Mo- $K_{\alpha}$  ( $\lambda$  = 0.71073 Å) radiation at 100(2) K. The data were corrected for absorption. The structures were solved by SIR-97 expanded by Fourier-difference syntheses, and refined with the SHELXL-97 package incorporated in WinGX 1.64 crystallographic package.<sup>[25]</sup> The position of the hydrogen atoms were calculated by assuming ideal geometries, but not refined. All non-hydrogen atoms were refined with anisotropic thermal parameters by full-matrix least-squares procedures on  $F^2$ . The convergence was measured by the factors  $R_1$  and  $R_2$ , where  $R_1 = \Sigma(|F_o| - |F_c|)/\Sigma|F_o|$  and  $R_2 = \{\Sigma[w(F_o^2 - F_c^2)^2]/\Sigma[w(F_o^2)^2]\}^{1/2}$ . For complex **2**, the Cl1 atom is disordered over two positions (Cl1A and Cl1B), which was refined with a site occupa-

tion factor of 0.5. Selected bond lengths and angles are listed in Table 1. Pertinent crystallographic parameters for complexes **1–3** are summarized in Table 2. Figure 3b was generated using the DIAMOND package.<sup>[26]</sup>

**Table 1.** Selected bond lengths (Å) and angles (°) for [Cu<sup>II</sup><sub>2</sub>(L<sup>6</sup>)<sub>2</sub>( $\mu$ -Cl)(Cl)(Cu<sup>II</sup>Cl<sub>4</sub>)] (**1**), [Cu<sup>II</sup>(L<sup>6</sup>)( $\mu$ -Cl)] [ClO<sub>4</sub>] $\cdot$ CH<sub>3</sub>CN (**2**) and [Cu<sup>II</sup><sub>2</sub>(L<sup>7</sup>)<sub>2</sub>( $\mu$ -Cl)<sub>2</sub>] [ClO<sub>4</sub>]<sub>2</sub> (**3**).

[Cu <sup>II</sup> (L <sup>6</sup> ) <sub>2</sub> ( $\mu$ -Cl)(Cl)(Cu <sup>II</sup> Cl <sub>4</sub> )] ( <b>1</b> )			
Cu1–N1	2.129(4)	N1–Cu1–N2	90.99(16)
Cu1–N2	1.987(4)	N1–Cu1–N4	81.31(17)
Cu1–N4	1.958(4)	N2–Cu1–N4	167.34(18)
Cu1–Cl1	2.2795(13)	N1–Cu1–Cl1	163.40(12)
Cu1–Cl2	2.6448(13)	N1–Cu1–Cl2	100.56(11)
Cu2–N5	2.130(4)	N2–Cu1–Cl1	92.85(12)
Cu2–N6	1.966(4)	N2–Cu1–Cl2	94.68(12)
Cu2–N7	1.959(4)	N4–Cu1–Cl1	91.84(13)
Cu2–Cl2	2.3348(12)	N4–Cu1–Cl2	96.60(13)
Cu2–Cl3	2.6482(13)	Cl1–Cu1–Cl2	95.22(5)
Cu3–Cl3	2.2957(13)	N5–Cu2–N6	92.03(16)
Cu3–Cl4	2.2512(13)	N5–Cu2–N7	80.81(16)
Cu3–Cl5	2.2134(13)	N6–Cu2–N7	169.85(16)
Cu3–Cl6	2.2603(13)	N5–Cu2–Cl2	166.66(12)
Cu1...Cu2	4.0169(10)	N5–Cu2–Cl3	100.09(11)
Cu2...Cu3	4.3394(12)	N6–Cu2–Cl2	93.87(12)
		N6–Cu2–Cl3	96.79(12)
		N7–Cu2–Cl2	91.70(12)
		N7–Cu2–Cl3	91.57(12)
		Cl2–Cu2–Cl3	91.09(4)
		Cl3–Cu3–Cl4	98.89(5)
		Cl3–Cu3–Cl5	101.88(5)
		Cl3–Cu3–Cl6	122.93(5)
		Cl4–Cu3–Cl5	129.27(5)
		Cl4–Cu3–Cl6	101.94(5)
		Cl5–Cu3–Cl6	104.39(5)
		Cu1–Cl2–Cu2	107.38(5)
		Cu2–Cl3–Cu3	122.58(5)
[Cu <sup>II</sup> (L <sup>6</sup> )( $\mu$ -Cl)] [ClO <sub>4</sub> ] $\cdot$ CH <sub>3</sub> CN ( <b>2</b> )			
Cu1–N1	2.057(7)	N1–Cu1–N2	96.2(2)
Cu1–N2	2.027(5)	N1–Cu1–N3	80.0(2)
Cu1–N3	1.985(7)	N2–Cu1–N3	176.1(3)
Cu1–Cl1A <sub>eq</sub>	2.255(7)	N1–Cu1–Cl1A	164.3(5)
Cu1–Cl1B <sub>eq</sub>	2.278(8)	N1–Cu1–Cl1B	162.2(5)
Cu1–Cl1A <sub>#ax</sub>	2.823(14)	N2–Cu1–Cl1A	96.3(3)
Cu1–Cl1B <sub>#ax</sub>	2.822(14)	N2–Cu1–Cl1B	95.9(3)
Cu1...Cu1#	3.984(4)	N3–Cu1–Cl1A	87.3(3)
		N3–Cu1–Cl1B	88.1(3)
		Cu1–Cl1A–Cu1#	102.8(3)
		Cu1–Cl1B–Cu1#	102.2(4)
[Cu <sup>II</sup> <sub>2</sub> (L <sup>7</sup> ) <sub>2</sub> ( $\mu$ -Cl) <sub>2</sub> ] [ClO <sub>4</sub> ] <sub>2</sub> ( <b>3</b> )			
Cu1–N1	1.977(4)	N1–Cu1–N3	79.3(2)
Cu1–N3	2.085(4)	N1–Cu1–N4	172.7(2)
Cu1–N4	1.993(4)	N3–Cu1–N4	93.4(2)
Cu1–Cl1	2.286(1)	N1–Cu1–Cl1	90.9(1)
Cu1–Cl1#	2.732(1)	N3–Cu1–Cl1	162.7(1)
Cu1...Cu1#	3.503(3)	N4–Cu1–Cl1	96.4(1)
		N1–Cu1–Cl1#	89.3(1)
		N3–Cu1–Cl1#	102.1(1)
		N4–Cu1–Cl1#	91.13(1)
		Cu1–Cl1–Cu1#	88.09(4)

Symmetry transformations used to generate equivalent atoms: **2:** # 1.5+x, 1–y, 1–z. **3:** 1 –x, –y, 2–z.

Crystallographic data (excluding structure factors) for the structures in this paper have been deposited with the Cambridge Crystallographic

**Table 2.** Data collection and structure refinement parameters for  $[\text{Cu}_2^{\text{II}}(\text{L}^6)_2(\mu\text{-Cl})(\text{Cl})(\text{Cu}^{\text{II}}\text{Cl}_4)]$  (**1**),  $[\text{Cu}^{\text{II}}(\text{L}^6)(\mu\text{-Cl})][\text{ClO}_4]\cdot\text{CH}_3\text{CN}$  (**2**),  $[\text{Cu}^{\text{II}}_2(\text{L}^7)_2(\mu\text{-Cl})_2][\text{ClO}_4]_2$  (**3**).

	1	2	3
Formula	$\text{C}_{24}\text{H}_{32}\text{Cl}_6\text{Cu}_3\text{N}_8$	$\text{C}_{14}\text{H}_{19}\text{Cl}_2\text{CuN}_5\text{O}_4$	$\text{C}_{36}\text{H}_{40}\text{Cl}_4\text{Cu}_2\text{N}_8\text{O}_{10}$
MW / $\text{g}\cdot\text{mol}^{-1}$	835.90	455.78	981.64
Crystal color, habit	green, block	blue, block	blue, block
$T/\text{K}$	100(2)	100(2)	100(2)
$\lambda/\text{\AA}$	Mo- $K_\alpha$ (0.71073)	Mo- $K_\alpha$ (0.71073)	Mo- $K_\alpha$ (0.71073)
Crystal system	triclinic	orthorhombic	monoclinic
Space group	$P\bar{1}$ (no. 2)	$P2_1cn$ (no. 33)	$P2_1/n$ (no. 14)
$a/\text{\AA}$	9.1576(14)	6.5723(18)	11.7516(16)
$b/\text{\AA}$	13.360(2)	11.185(3)	13.1571(18)
$c/\text{\AA}$	15.001(2)	25.092(7)	14.1066(19)
$\alpha/^\circ$	65.383(2)	90.0	90.0
$\beta/^\circ$	78.100(2)	90.0	113.031(2)
$\gamma/^\circ$	71.173(2)	90.0	90.0
$V/\text{\AA}^3$	1573.7(4)	1844.6(9)	2007.3(5)
<b>Z</b>	2	4	2
$D_{\text{calcd.}}/\text{g}\cdot\text{cm}^{-3}$	1.764	1.641	1.624
$\mu/\text{mm}^{-1}$	2.5490	2.504	1.388
Reflections measured	8398	8944	12831
Unique reflections ( $R_{\text{int}}$ )	5709 (0.0237)	3363 (0.0764)	4952 (0.0491)
Reflections used	4729	2402	3678
$[I > 2\sigma(I)]$			
$R_1, wR_2$	$R_1 = 0.0464$	$R_1 = 0.0759$	$R_1 = 0.0663$
$[I > 2\sigma(I)]$	$wR_2 = 0.1272$	$wR_2 = 0.1999$	$wR_2 = 0.1840$
$R_1, wR_2$ (all data)	$R_1 = 0.0592$	$R_1 = 0.1053$	$R_1 = 0.0999$
	$wR_2 = 0.1643$	$wR_2 = 0.2389$	$wR_2 = 0.2858$

Data Centre, CCDC, 12 Union Road, Cambridge CB21EZ, UK. Copies of the data can be obtained free of charge on quoting the depository numbers CCDC-978949 for **1**, CCDC-978950 for **2**, and CCDC-978951 for **3** (Fax: +44-1223-336-033; E-Mail: deposit@ccdc.cam.ac.uk, <http://www.ccdc.cam.ac.uk>)

**Supporting Information** (see footnote on the first page of this article):  $^1\text{H}$  NMR spectra of  $\text{L}^6$  and  $\text{L}^7$ , UV/Vis spectra of **1–3**.

## Results and Analysis

### Syntheses of Ligands and Complexes

Two new ligands  $\text{L}^6$  and  $\text{L}^7$  were synthesized by condensation of pyrazole-1-carbinol with *N*-methyl-2-aminoethyl-2-pyridine and *N*-benzyl-2-(pyridin-2-yl)ethanamine, respectively, in the presence of anhydrous  $\text{Na}_2\text{CO}_3$  in dry acetonitrile. Ligands were characterized by their  $^1\text{H}$  NMR spectra, displayed in Figures S1 and S2 (Supporting Information), respectively. The complex  $[\text{Cu}^{\text{II}}_2(\text{L}^6)_2(\mu\text{-Cl})(\text{Cl})(\text{Cu}^{\text{II}}\text{Cl}_4)]$  (**1**) was synthesized from the reaction between  $\text{L}^6$  and  $\text{Cu}^{\text{II}}\text{Cl}_2\cdot 2\text{H}_2\text{O}$  (2:3 molar ratio) in acetonitrile. The coordination polymer  $[\text{Cu}^{\text{II}}(\text{L}^6)(\mu\text{-Cl})][\text{ClO}_4]\cdot\text{CH}_3\text{CN}$  (**2**) and the discrete dimer  $[\text{Cu}^{\text{II}}_2(\text{L}^7)_2(\mu\text{-Cl})_2][\text{ClO}_4]_2$  (**3**) were prepared by the reaction of  $\text{Cu}^{\text{II}}\text{Cl}_2\cdot 2\text{H}_2\text{O}$  in stoichiometric ratio with  $\text{L}^6$  and  $\text{L}^7$ , respectively, in the presence of excess sodium perchlorate.

Complexes **2** and **3** display characteristic IR spectral absorptions at ca.  $1100\text{ cm}^{-1}$  and  $600\text{ cm}^{-1}$ , due to  $\nu(\text{ClO}_4^-)$  stretching vibration. The electronic spectra of **1–3** recorded in acetonitrile are displayed in Figures S3–S5 (Supporting Information), respectively. Crystal-field transitions for these complexes were observed in the range 620–700 nm, attesting their square-py-

ramidal arrangement.<sup>[21]</sup> Higher energy transitions in the range 260–285 nm are due to metal-perturbed intraligand transitions.

### Structural Analysis. Structure of $[\text{Cu}_2^{\text{II}}(\text{L}^6)_2(\mu\text{-Cl})(\text{Cl})(\text{Cu}^{\text{II}}\text{Cl}_4)]$ (**1**)

To confirm the structure of the complexes and mode of coordination of the terminal ligands  $\text{L}^6$  and  $\text{L}^7$  and the bridging ligands, single-crystal X-ray structure determination of **1–3** was carried out. Selected bond lengths and bond angles are listed in Table 1.

A perspective view of the crystal structure of  $[\text{Cu}_2^{\text{II}}(\text{L}^6)_2(\mu\text{-Cl})(\text{Cl})(\text{Cu}^{\text{II}}\text{Cl}_4)]$  is shown in Figure 2. The tridentate ligand  $\text{L}^6$  is coordinated to the  $\text{Cu}^{\text{II}}$  in a meridional mode. The arrangement around copper(II) is distorted square-pyramidal for Cu1 and Cu2 and distorted tetrahedral for Cu3. The  $\tau$  values are 0.06 and 0.05 for Cu1 and Cu2, respectively, indicating that the environment around these two central copper(II) atoms is nearly perfect square-pyramidal.<sup>[27]</sup> The equatorial plane around Cu1 consists of a tertiary amine nitrogen N1, a pyridyl nitrogen N2, pyrazole nitrogen N4, and a terminal chloride Cl1. The apical site is occupied by a bridging chloride Cl2, which is in the equatorial plane of the neighboring Cu2 ion. Three basal sites for Cu2 are occupied by three donor atoms N5, N6, and N7 of  $\text{L}^6$ . The axial site of Cu2 is occupied by another bridging chloride ion, provided by a  $[\text{Cu}^{\text{II}}\text{Cl}_4]^{2-}$  unit. It is observed that the average  $\text{Cu}-\text{Cl}_{\text{ax}}$  (ax = axial) distance is larger than the  $\text{Cu}-\text{Cl}_{\text{eq}}$  (eq = equatorial) distance, which is typical for copper(II) square-pyramidal complexes due to Jahn-Teller distortion of the copper(II) ion [ $\text{Cu}-\text{Cl}_{2,\text{ax}}$  2.6448(13) Å,  $\text{Cu}-\text{Cl}_{1,\text{eq}}$  2.2795(13) Å for Cu1 and  $\text{Cu}-\text{Cl}_{3,\text{ax}}$  2.6482(13) Å,



Cu–Cl1<sub>eq</sub> 2.3348(12) Å for Cu2]. The average Cu–N<sub>pz</sub> (pz = pyrazole) distance is shorter than that of Cu–N<sub>py</sub> (py = pyridine) [Cu–N<sub>pz</sub> 1.958(4) Å, Cu–N<sub>py</sub> 1.987(4) Å]. The Cu–N<sub>am</sub> (am = amine) bond lengths [2.129(4) Å for Cu1 and 2.130(4) Å for Cu2] are appreciably longer than Cu–N<sub>pz</sub> and Cu–N<sub>py</sub> distances. The Cu1 and Cu2 ions are positioned out of equatorial plane towards Cl2 by 0.244 Å and Cl3 by 0.183 Å, respectively. The tetrahedral site around the central Cu3 atom is occupied by three terminal chloride ions Cl4, Cl5, and Cl6 and a bridging chloride ion Cl3. The angles around the Cu3 atom are varying from 98.89(5)° to 129.27(5)°. The Cu1...Cu2 and Cu2...Cu3 distances are 4.0169(10) Å and 4.3394(12) Å, respectively. The Cu1–Cl2–Cu2 and Cu2–Cl3–Cu3 bridging angles are 107.38(5)° and 122.58(5)°, respectively.

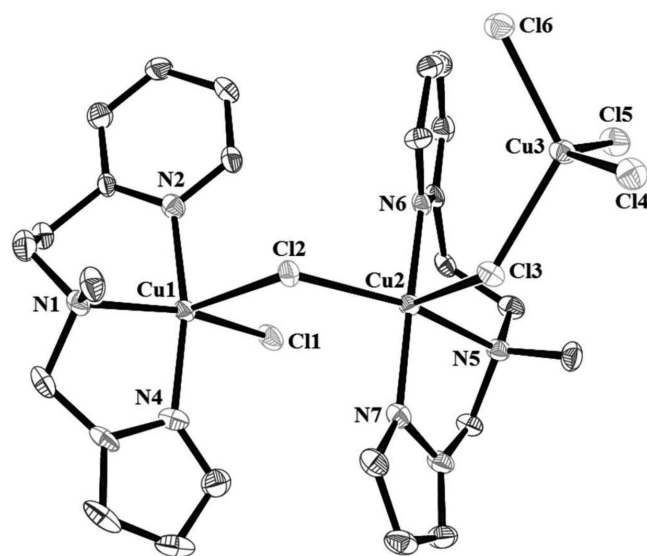


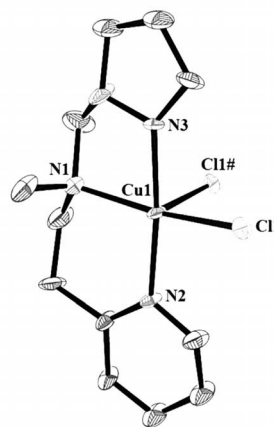
**Figure 2.** Perspective view of the cationic part of  $[\text{Cu}_2^{\text{II}}(\text{L}^6)_2(\mu\text{-Cl})(\text{Cl})]$  ( $\text{Cu}^{\text{II}}\text{Cl}_4$ ) (1). All hydrogen atoms are omitted for clarity.

### Structure of $[\text{Cu}^{\text{II}}(\text{L}^6)(\mu\text{-Cl})][\text{ClO}_4]\cdot\text{CH}_3\text{CN}$ (2)

The asymmetric unit contains the mononuclear unit “ $\text{Cu}^{\text{II}}(\text{L}^6)(\text{Cl})$ ”, one perchlorate anion, and an acetonitrile molecule as solvent of crystallization. Notably, the Cl1 atom is disordered over two positions Cl1A and Cl1B. A perspective view of the cationic part of the crystal of  $[\text{Cu}^{\text{II}}(\text{L}^6)(\mu\text{-Cl})][\text{ClO}_4]\cdot\text{CH}_3\text{CN}$  is shown in Figure 3, with the presence of only Cl1A. In the subsequent discussion only Cl1A is considered, as metric parameters associated with Cl1A and Cl1B are closely similar. The tridentate ligand  $\text{L}^6$  coordinates to  $\text{Cu}^{\text{II}}$  in a meridional mode, as in complex 1. Axial coordination is provided by a chloride ion from a neighboring molecule. In the mononuclear unit, the coordination polyhedron around the copper(II) ion can be best described as distorted square-pyramidal ( $\tau = 0.17$ ).<sup>[27]</sup> The basal plane is completed by the tertiary amine nitrogen N1, pyridyl nitrogen N2, pyrazole nitrogen N3, and the chloride ion Cl1A. The chloride ion Cl1A# acts as a bridge and is occupied at the apical position of the symmetry-related central copper(II) atoms (Figure 3a). This coordination eventually leads to the formation of a 1D polymeric chain (Fig-

ure 3b). The Cu1–Cl1A#<sub>ax</sub> distance is greater than Cu1–Cl1A<sub>eq</sub> distance [Cu1–Cl1A#<sub>ax</sub> 2.823(14) Å, Cu1–Cl1<sub>eq</sub> 2.255(7) Å]. The Cu1–N<sub>pz</sub> distance is shorter than that of Cu1–N<sub>py</sub> [Cu1–N<sub>pz</sub> 1.985(7), Cu1–N<sub>py</sub> 2.027(5) Å]. The Cu–N<sub>am</sub> bond length 2.057(7) Å is appreciably longer than Cu1–N<sub>pz</sub> and Cu1–N<sub>py</sub> bond lengths. The central copper(II) atom is positioned out of the equatorial plane towards Cl1A# by 0.188 Å. The separation between Cu1...Cu1# along the chain is 3.984(4) Å. The Cu1–Cl1A#–Cu1# bridging angle is 102.8(3)°.

(a)



(b)

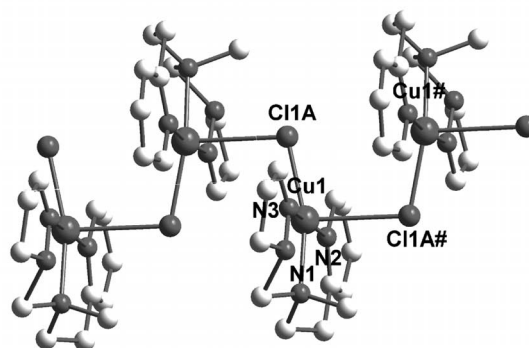


**Figure 3.** (a) Perspective view of the cationic part of  $[\text{Cu}^{\text{II}}(\text{L}^6)(\mu\text{-Cl})][\text{ClO}_4]\cdot\text{CH}_3\text{CN}$  (2). All hydrogen atoms are omitted for clarity. (b) 1D polymeric chain of  $[\text{Cu}^{\text{II}}(\text{L}^6)(\mu\text{-Cl})][\text{ClO}_4]\cdot\text{CH}_3\text{CN}$  (2). All hydrogen atoms are omitted for clarity.

### Structure of $[\text{Cu}^{\text{II}}_2(\text{L}^7)_2(\mu\text{-Cl})_2][\text{ClO}_4]_2$ (3)

A perspective view of the cationic part of the complex is displayed in Figure 4. The complex consists of a discrete  $[\text{Cu}^{\text{II}}_2(\text{L}^7)_2(\mu\text{-Cl})_2]^{2+}$  unit. The two mononuclear units are related by a crystallographic center of symmetry. Each  $\text{Cu}^{\text{II}}$  atom is in distorted square-pyramidal coordination environment with trigonality index parameter  $\tau = 0.16$ .<sup>[27]</sup> A bridging chloride ion Cl1, pyrazole nitrogen N1, a tertiary amine N3, and pyridyl nitrogen N4 comprise the basal plane. The apical site is occupied by bridging chloride Cl1#, which is in the equatorial plane of a neighboring Cu1# atom. The ligand  $\text{L}^7$  coordinates to  $\text{Cu}^{\text{II}}$

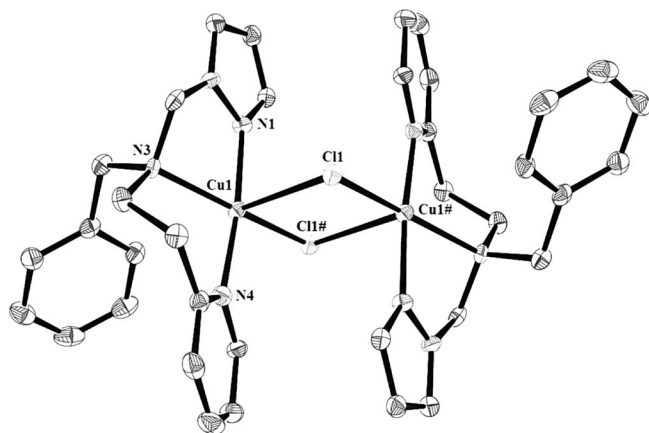


**Figure 4.** Perspective view of the cationic part of  $[\text{Cu}_2^{\text{II}}(\text{L}^7)_2(\mu\text{-Cl})_2][\text{ClO}_4]_2$  (**3**). All hydrogen atoms are omitted for clarity.

in the meridional mode, as that  $\text{L}^6$  in complexes **1** and **2**. The  $\text{Cu1-Cl}_{\text{ax}}$  distance is appreciably longer than  $\text{Cu1-Cl}_{\text{eq}}$  distance [ $\text{Cu1-Cl1}_{\text{ax}}$  2.732(1),  $\text{Cu1-Cl1}_{\text{eq}}$  2.286(1) Å]. The  $\text{Cu1-N}_{\text{pz}}$  distance is shorter than that of  $\text{Cu1-N}_{\text{py}}$  [ $\text{Cu1-N}_{\text{pz}}$  1.977(4),  $\text{Cu1-N}_{\text{py}}$  1.993(4) Å]. The  $\text{Cu-N}_{\text{am}}$  bond length [ $\text{Cu1-N}_{\text{am}}$  2.085(4) Å] is appreciably longer than  $\text{Cu1-N}_{\text{pz}}$  and  $\text{Cu1-N}_{\text{py}}$ . The central copper(II) atom is displaced by 0.133 Å from the least-squares plane defined by the  $\text{N}_3\text{Cl}$  basal plane towards the bridging chloride  $\text{Cl1\#}$ . The  $\text{Cu1-Cl1-Cu1\#}$  bridging angle is 88.09(4)°. The  $\text{Cu1}\cdots\text{Cu1\#}$  distance 3.503(3) Å.

**Magnetic Properties of  $[\text{Cu}_2^{\text{II}}(\text{L}^6)_2(\mu\text{-Cl})(\text{Cl})(\text{Cu}^{\text{II}}\text{Cl}_4)]$  (**1**),  $[\text{Cu}^{\text{II}}(\text{L}^6)(\mu\text{-Cl})][\text{ClO}_4]\cdot\text{CH}_3\text{CN}$  (**2**), and  $[\text{Cu}^{\text{II}}_2(\text{L}^7)_2(\mu\text{-Cl})_2][\text{ClO}_4]_2$  (**3**)**

Magnetic susceptibility measurements of the powdered samples of **1–3** were carried out in the temperature range 2–300 K. For complex **1**, the  $\chi_{\text{M}}T$  value at 300 K is  $1.30 \text{ cm}^3\cdot\text{K}\cdot\text{mol}^{-1}$  ( $\mu_{\text{eff}}/\text{Cu} = 1.86 \mu_{\text{B}}$ ). The  $\chi_{\text{M}}T$  values are almost constant over the temperature range 50–300 K. The  $\chi_{\text{M}}T$  values decrease very slightly with decreasing temperature to reach  $1.19 \text{ cm}^3\cdot\text{K}\cdot\text{mol}^{-1}$  at 2 K, indicating the presence of very weak antiferromagnetic interaction between the  $\text{Cu}^{\text{II}}$  ions (Figure 5). The variation of the  $\chi_{\text{M}}T$  values is so small that any model [both intramolecular (dimer or trimer) as intermolecular] can reproduce the experimental data, precluding an unambiguous knowledge of the pathway responsible of this weak magnetic interaction. In this sense, the experimental data were fit by using the Curie-Weiss law. The best-fit parameters are  $\theta = -0.19(1) \text{ K}$  and  $g = 2.07(1)$ , where  $\theta$  is the parameter, which takes into account antiferromagnetic interactions between the paramagnetic  $\text{Cu}^{\text{II}}$  ions. The small negative Weiss constant indicates the very weak antiferromagnetic interaction which, in principle, can be attributed to  $\text{Cu}(1)\text{--Cl}(2)\text{--Cu}(2)$  and/or  $\text{Cu}(2)\text{--Cl}(3)\text{--Cu}(3)$  and/or intermolecular pathways (see Figure 2).

The magnetic behavior of **2** is illustrated in Figure 6. The value of  $\chi_{\text{M}}T$  is  $0.42 \text{ cm}^3\cdot\text{K}\cdot\text{mol}^{-1}$  at 300 K ( $\mu_{\text{eff}}/\text{Cu} = 1.83 \mu_{\text{B}}$ ) and the values are almost constant over the temperature range 50–300 K. Then the values decrease rapidly to  $0.36 \text{ cm}^3\cdot\text{K}\cdot\text{mol}^{-1}$  at 2 K. This indicates that there exists antiferromagnetic coupling between the  $\text{Cu}^{\text{II}}$  atoms. The experimentally observed  $\chi_{\text{M}}$  values were fitted using the numerical expression [Equation (1)] for a regular antiferromagnetic single-chain polymer.<sup>[18g,28]</sup> The best-fit parameters obtained are  $J = -0.20(1) \text{ cm}^{-1}$  and  $g = 2.11$ .

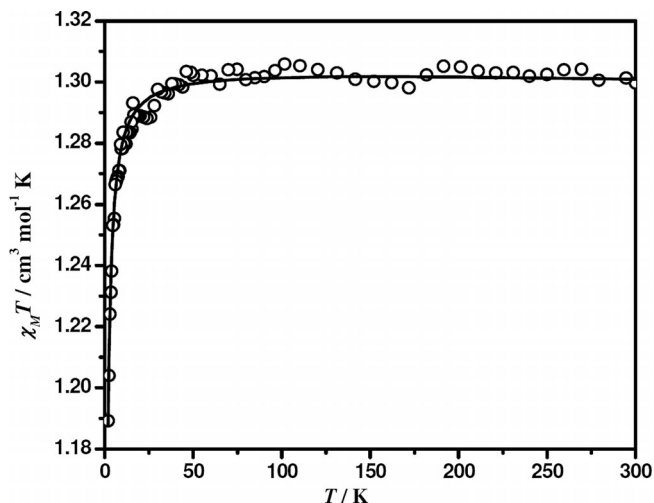


**Figure 5.** Plot of  $\chi_{\text{M}}T$  vs.  $T$  for a powdered sample of  $[\text{Cu}_2^{\text{II}}(\text{L}^6)_2(\mu\text{-Cl})(\text{Cl})(\text{Cu}^{\text{II}}\text{Cl}_4)]$  (**1**).

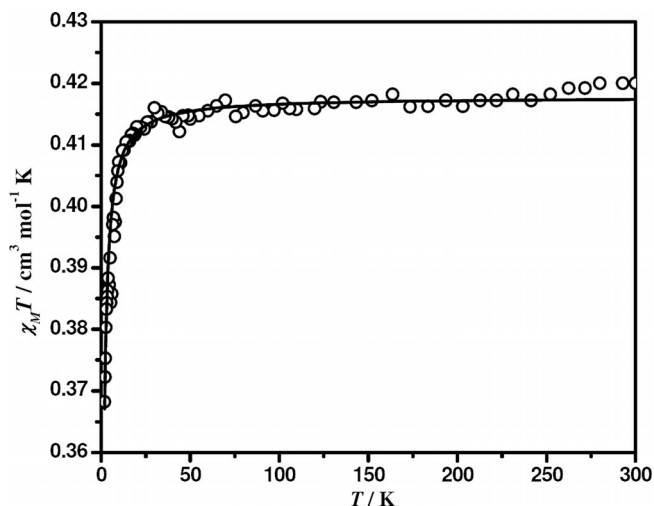


**Figure 6.** Plot of  $\chi_{\text{M}}T$  vs.  $T$  for a powdered sample of  $[\text{Cu}^{\text{II}}(\text{L}^6)(\mu\text{-Cl})][\text{ClO}_4]\cdot\text{CH}_3\text{CN}$  (**2**).

$\text{K}\cdot\text{mol}^{-1}$  at 2 K. This indicates that there exists antiferromagnetic coupling between the  $\text{Cu}^{\text{II}}$  atoms. The experimentally observed  $\chi_{\text{M}}$  values were fitted using the numerical expression [Equation (1)] for a regular antiferromagnetic single-chain polymer.<sup>[18g,28]</sup> The best-fit parameters obtained are  $J = -0.20(1) \text{ cm}^{-1}$  and  $g = 2.11$ .

$$\chi_{\text{M}} = (N\beta^2 g^2 / kT) A/B \quad (1)$$

$$A = 0.25 + 0.074975x + 0.075235x^2$$

$$B = 1 + 0.9931x + 0.172135x^2 + 0.757825x^3$$

$$x = J/kT$$

For complex **3** the value of  $\chi_{\text{M}}T$  at 300 K is  $0.82 \text{ cm}^3\cdot\text{K}\cdot\text{mol}^{-1}$  ( $\mu_{\text{eff}}/\text{Cu} = 1.81 \mu_{\text{B}}$ ) and upon cooling the value increases and reaches a maximum of  $0.95 \text{ cm}^3\cdot\text{K}\cdot\text{mol}^{-1}$  at  $T = 6 \text{ K}$ . This behavior is due to ferromagnetic coupling between the  $\text{Cu}^{\text{II}}$

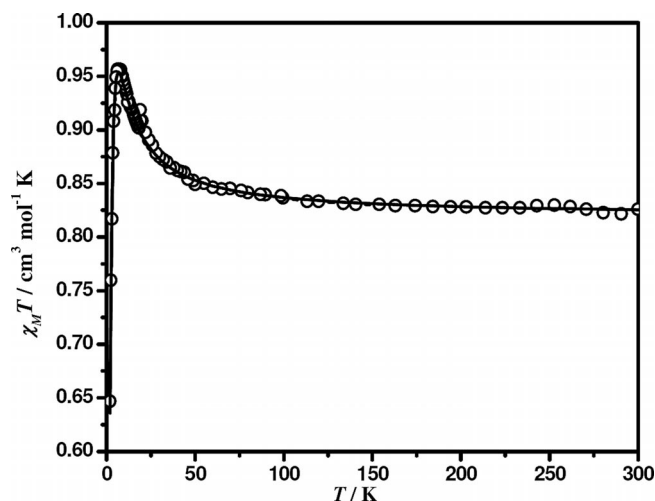


**Figure 7.** Plot of  $\chi_M T$  vs.  $T$  for a powdered sample of  $[(L^7)_2Cu^{II}_2(\mu-Cl)_2][ClO_4]_2$  (**3**).

atoms. A plot of  $\chi_M T$  vs.  $T$  is presented in Figure 7. Below 6 K, the  $\chi_M T$  value decreases, indicating the presence of anti-ferromagnetic intermolecular interactions and/or zero-field splitting. The experimental data were fitted by using the modified expression [Equation (2)] for two interacting  $S = 1/2$  centers,<sup>[1]</sup> developed under the usual isotropic (Heisenberg) exchange Hamiltonian  $\hat{H} = -JS_1 \cdot S_2$ . The best-fitting for experimental data leads to the parameters:  $J = +6.0(1) \text{ cm}^{-1}$ ,  $D$  (zero-field splitting parameter) =  $4.5(2) \text{ cm}^{-1}$  and  $g = 2.11$ . The solid line in Figure 7 corresponds to the best theoretical fit.

$$\chi_M = \frac{(2N\beta^2 g^2 / kT) \exp(-D/3kT) [\exp(-2D/3kT) + 2 \exp(-D/3kT) + \exp(-J/kT)]^{-1}}{(2)} \quad (2)$$

The positive value of  $J$  reveals a ferromagnetic interaction between the  $Cu^{II}$  ions. The observed result is due to the bridging mode present in **3**: a chloride ion that occupies a basal coordination site in one  $Cu^{II}$  atom occupies an apical position in the coordination sphere of the neighboring  $Cu^{II}$  atom (see Figure 4).

## Discussion

The five-coordinate chloro-bridged dinuclear copper(II) complexes with square-pyramids sharing a base-to-apex edge with parallel basal planes usually show small ferromagnetic or antiferromagnetic coupling constants  $J$ .<sup>[16,18c,18d]</sup> Theoretical calculations show that the  $d_{x^2-y^2}$  orbital of Cu is used for a  $\sigma^*$  interaction with the  $p_N$  and  $p_{Cl}$  orbitals of the basal plane ligands.<sup>[18c,18d]</sup> The HOMO is an antisymmetric combination of  $d_{Cu}-d_{Cu}$  orbitals, whereas the LUMO is the symmetric one (Figure 8). The superexchange pathway will take place mainly through a  $\pi^*$  type of interaction between the Cu  $d_{x^2-y^2}$  and the apical  $p_{Cl}$  orbitals. For an ideal square  $Cu^{II}(\mu-Cl)_2Cu^{II}$  core the overlap integral for such an interaction would be zero. Hence, there would be no magnetic coupling between the central copper(II) atoms. Deviation from orthogonality facilitates the overlap of magnetic orbitals and thereby increases antiferromagnetic interaction.

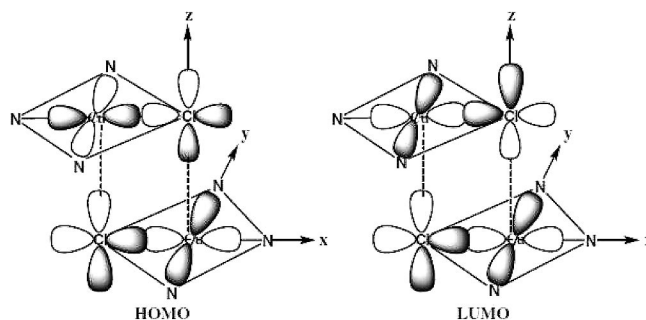


**Figure 8.** Schematic presentation of HOMO and LUMO for parallel-planar  $Cu^{II}(\mu-Cl)_2Cu^{II}$  dimers.

By now the structure of a large variety of mono-chloro- and di-chloro-bridged copper(II) complexes has been determined, aiming at correlating their structures and magnetic properties. Various structural parameters have been considered in the pursuit of identifying systematic magneto-structural variations. For five-coordinate di-chloro-bridged copper(II) complexes with the bridging ligands occupying apical and equatorial sites of each  $Cu^{II}$  ion, Hatfield<sup>[16b]</sup> provided a correlation between the  $J$  (singlet-triplet energy gap) and the structural parameter  $\phi/R$  ( $\text{deg} \cdot \text{\AA}^{-1}$ ), where  $\phi$  is the Cu–Cl–Cu bridge angle and  $R$  is the Cu–Cl long bond length. Antiferromagnetic coupling is observed for values of  $\phi/R$  below  $32.6$  ( $\text{deg} \cdot \text{\AA}^{-1}$ ) or above  $34.8$  ( $\text{deg} \cdot \text{\AA}^{-1}$ ), while ferromagnetic exchange is found for the values of  $\phi/R$  falling between these limits. In  $[(L^7)_2Cu^{II}_2(\mu-Cl)_2][ClO_4]_2$  (**3**) two square-pyramids ( $\tau = 0.16$ ) share one base-to-apex edge with parallel basal plane and the value of  $\phi/R$  is  $32.2$  ( $\text{deg} \cdot \text{\AA}^{-1}$ ) (Table 1), which is very close to the reported range predicted to exhibit ferromagnetic exchange. Thus for complex **3** the observed ferromagnetic coupling  $J = +6.0(1) \text{ cm}^{-1}$  is consistent with this correlation.

Some correlations have been obtained between the magnetic and structural parameters for mono- $\mu$ -chloro-copper chains.<sup>[18e,18h]</sup> The magnetic and structural data are consistent with the reduced number of exchange pathways but the authors of these two reports caution that more data are required before the apparent magneto-structural correlation can be established. However, following these correlations, overall ferromagnetic behavior can be expected for values of the quotient  $\phi/R$  lower than approximately 40 and higher than 57, whereas antiferromagnetic character appears when this quotient  $\phi/R$  is between these two values.<sup>[18h]</sup> Complex **2** is a mono-chloro-bridged single-chain 1D coordination polymer, in which the bridging  $Cl^-$  ion occupies an equatorial position for one  $Cu^{II}$  atom and an axial position for symmetry-generated  $Cu^{II}$  atoms. The central copper(II) atom assumes closer to a square-pyramidal arrangement ( $\tau = 0.16$ ). For complex **2** the value of  $\phi/R$  is  $36.4 \text{ deg} \cdot \text{\AA}^{-1}$  and it shows antiferromagnetic coupling with  $J = -0.20(1) \text{ cm}^{-1}$ . According to literature prediction,<sup>[18h]</sup> complex **2** should exhibit ferromagnetic interaction. However, a qualitative relation between the ferro- or antiferro-magnetic behavior and  $\theta$  (Cl–Cu–L angle, L = ligand *trans* to Cl) has also been proposed.<sup>[18c,18d,18f,18i]</sup> It has been observed that  $\theta$  angles close to  $180^\circ$  favor the ferromagnetic behavior, whereas an antiferro-



magnetic behavior is observed for  $\theta$  angles smaller than  $167^\circ$ .<sup>[18f]</sup> For complex **2** the  $\theta$  value is  $164^\circ$  (Table 1). The observed antiferromagnetic behavior is thus justified.

Complex **1** is a trimer, which presents two different mono-chloro-bridges (Cu1–Cl2–Cu2 and Cu2–Cl3–Cu3), similar to **2** and **3**. In **1** the Cu1 and Cu2 atoms present a nearly perfect square-pyramidal arrangement ( $\tau$  values are 0.06 and 0.05, respectively) and its value of  $\phi/R$  is  $40.5 \text{ deg} \cdot \text{\AA}^{-1}$ , whereas Cu3 presents a distorted tetrahedral environment and its  $\phi/R$  value is  $46.3 \text{ deg} \cdot \text{\AA}^{-1}$ . For both pathways an antiferromagnetic interaction is expected, although for the last one no predictions can be made due to the tetrahedral arrangement of Cu3. So, given the weak antiferromagnetic interaction observed for **1**, we may attribute it to the Cu1–Cl2–Cu2 pathway.

## Summary and Conclusions

The chloro-bridged Cu<sup>II</sup> complexes [Cu<sub>2</sub><sup>II</sup>(L<sup>6</sup>)<sub>2</sub>(μ-Cl)(Cl)(Cu<sup>II</sup>Cl<sub>4</sub>)] (**1**) [Cu<sup>II</sup>(L<sup>6</sup>)(μ-Cl)][ClO<sub>4</sub>] $\cdot$ CH<sub>3</sub>CN (**2**), and [Cu<sup>II</sup><sub>2</sub>(L<sup>7</sup>)<sub>2</sub>(μ-Cl)<sub>2</sub>][ClO<sub>4</sub>]<sub>2</sub> (**3**) were synthesized by using pyridine- and pyrazole-based tridentate ligands L<sup>6</sup> and L<sup>7</sup>. Complex **2** presents a chain structure via equatorial-apical chloride bridges, whereas complex **3** is a di-chloro-bridged dinuclear complex, where each bridging chloride simultaneously occupies an in-plane coordination site on one Cu<sup>II</sup> ion and an apical site on the other Cu<sup>II</sup> ion. Using a common tridentate ligand L<sup>6</sup> but differing in the synthetic procedure afforded two copper(II) complexes with different structure types **1** (mono-chloro-bridged copper(II) dimer with terminally coordination Cu<sup>I</sup>–Cl<sub>4</sub><sup>2–</sup> ion) and **2** (1D copper(II) chain). While the complexes **1** and **2** show weak antiferromagnetic coupling, complex **3** exhibits ferromagnetic coupling between the central Cu<sup>II</sup> atoms. The magnetic properties of complexes **2** and **3** are structurally correlated with reported complexes in the literature.

## Acknowledgements

This work is supported by the Department of Science & Technology, Government of India. RM sincerely thanks DST for J. C. Bose fellowship. RS gratefully acknowledge the award of SRF by Council of Scientific & Industrial Research, Government of India.

## References

- [1] O. Kahn, *Molecular Magnetism*; VCH Publishers: New York, 1993.
- [2] a) O. Kahn, *Angew. Chem. Int. Ed. Engl.* **1985**, *24*, 834–850; b) O. Kahn, *Acc. Chem. Res.* **2000**, *33*, 647–657.
- [3] J. S. Miller, A. J. Epstein, *Angew. Chem. Int. Ed. Engl.* **1994**, *33*, 385–415.
- [4] a) D. J. Hodgson, *Prog. Inorg. Chem.* **1975**, *19*, 173–241; b) M. Melnik, *Coord. Chem. Rev.* **1981**, *36*, 1–44; c) M. Melnik, *Coord. Chem. Rev.* **1982**, *42*, 259–293; d) M. Kato, Y. Muto, *Coord. Chem. Rev.* **1988**, *92*, 45–83; e) L. K. Thompson, S. S. Tandon, *Comments Inorg. Chem.* **1996**, *18*, 125–144; f) J. Ribas, A. Escuer, M. Monfort, R. Vicente, R. Cortés, L. Lezama, T. Rojo, *Coord. Chem. Rev.* **1999**, *193–195*, 1027–1068; g) J. Ribas, A. Escuer, M. Monfort, R. Vicente, R. Cortés, L. Lezama, T. Rojo, *Coord. Chem. Rev.* **1999**, *193–195*, 1027–1068; h) Y.-F. Zeng, X. Hu, F.-C. Liu, X.-H. Bu, *Chem. Soc. Rev.* **2009**, *38*, 469–480.
- [5] a) P. J. Hay, J. C. Thibault, R. Hoffmann, *J. Am. Chem. Soc.* **1975**, *97*, 4884–4899; b) O. Kahn, *Inorg. Chim. Acta* **1982**, *62*, 3–14; c) E. Ruiz, P. Alemany, S. Alvarez, J. Cano, *Inorg. Chem.* **1997**, *36*, 3683–3688; d) E. Ruiz, P. Alemany, S. Alvarez, J. Cano, *J. Am. Chem. Soc.* **1997**, *119*, 1297–1303; e) A. Rodríguez-Fortea, P. Alemany, S. Alvarez, E. Ruiz, *Inorg. Chem.* **2002**, *41*, 3769–3778; f) D. Venegas-Yazigi, D. Aravena, E. Spodine, E. Ruiz, S. Alvarez, *Coord. Chem. Rev.* **2010**, *254*, 2086–2095.
- [6] a) Y. Nishida, S. Kida, *Inorg. Chem.* **1988**, *27*, 447–452; b) V. Mishra, F. Lloret, R. Mukherjee, *Eur. J. Inorg. Chem.* **2007**, 2161–2170.
- [7] a) K. Koga, M. Ohtsubo, Y. Yamada, M. Koikawa, T. Tokii, *Chem. Lett.* **2004**, *33*, 1606–1607; b) V. Mishra, F. Lloret, R. Mukherjee, *Inorg. Chim. Acta* **2006**, *359*, 4053–4056.
- [8] a) V. McKee, M. Zvagulis, C. A. Reed, *Inorg. Chem.* **1985**, *24*, 2914–2919; b) H. P. Berends, D. W. Stephen, *Inorg. Chem.* **1987**, *26*, 749–754.
- [9] V. H. Crawford, H. W. Richardson, J. R. Wasson, D. J. Hodgson, W. E. Hatfield, *Inorg. Chem.* **1976**, *15*, 2107–2110.
- [10] a) A. K. Patra, M. Ray, R. Mukherjee, *Polyhedron* **2000**, *19*, 1423–1428; b) D. Ghosh, R. Mukherjee, *Inorg. Chem.* **1998**, *37*, 6597–6605; c) S. P. Foxon, D. Utz, J. Astner, S. Schindler, F. Thaler, F. W. Heinemann, G. Liehr, J. Mukherjee, V. Balamurugan, D. Ghosh, R. Mukherjee, *Dalton Trans.* **2004**, 2321–2328; d) J. Mukherjee, R. Mukherjee, *Dalton Trans.* **2006**, 1611–1621.
- [11] a) S. Mandal, V. Balamurugan, F. Lloret, R. Mukherjee, *Inorg. Chem.* **2009**, *48*, 7544–7556; b) H. Arora, S. K. Barman, F. Lloret, R. Mukherjee, *Inorg. Chem.* **2012**, *51*, 5539–5553.
- [12] a) T. Kawata, M. Yamanaka, S. Ohba, Y. Nishida, M. Nagamatsu, T. Tokii, M. Kato, O. W. Steward, *Bull. Chem. Soc. Jpn.* **1992**, *65*, 2739–2747; b) S. Meenakumari, S. K. Tiwari, A. R. Chakravarty, *J. Chem. Soc. Dalton Trans.* **1993**, 2175–2181; c) R. Gupta, R. Hotchandani, R. Mukherjee, *Polyhedron* **2000**, *19*, 1429–1435.
- [13] a) R. Gupta, S. Mukherjee, R. Mukherjee, *J. Chem. Soc. Dalton Trans.* **1999**, 4025–4030; b) A. Mukherjee, F. Lloret, R. Mukherjee, *Inorg. Chem.* **2008**, *47*, 4471–4480.
- [14] X.-H. Bu, M. Du, L. Zhang, Z.-L. Shang, R.-H. Zhang, M. Shionoya, *J. Chem. Soc. Dalton Trans.* **2001**, 729–735.
- [15] a) K. K. Nanda, L. K. Thompson, J. N. Bridson, K. Nag, *J. Chem. Soc. Chem. Commun.* **1994**, 1337–1338; b) L. K. Thompson, S. K. Mandal, S. S. Tandon, J. N. Bridson, M. K. Park, *Inorg. Chem.* **1996**, *35*, 3117–3125.
- [16] a) W. E. Marsh, W. E. Hatfield, D. J. Hodgson, *Inorg. Chem.* **1982**, *21*, 2679–2684; b) W. E. Marsh, K. C. Patel, W. E. Hatfield, D. J. Hodgson, *Inorg. Chem.* **1983**, *22*, 511–515.
- [17] a) J. Glerup, D. J. Hodgson, E. Pedersen, *Acta Chem. Scand. A* **1983**, *37*, 161–164; b) S. M. Gorun, S. J. Lippard, *Inorg. Chem.* **1991**, *30*, 1625–1630; c) N. A. Law, J. W. Kampf, V. L. Pecoraro, *Inorg. Chim. Acta* **2000**, *297*, 252–264; d) T. K. Karmakar, B. K. Ghosh, A. Usman, H.-K. Fun, E. Rivière, T. Mallah, G. Aromí, S. K. Chandra, *Inorg. Chem.* **2005**, *44*, 2391–2399.
- [18] a) T. Rojo, J. L. Mesa, M. I. Arriortua, J. M. Savariault, J. Galy, G. Villeneuve, D. Beltrán, *Inorg. Chem.* **1988**, *27*, 3904–3911; b) R. Cortés, L. Lezama, J. I. R. de Larramendi, G. Madariaga, J. L. Mesa, F. J. Zúñiga, T. Rojo, *Inorg. Chem.* **1995**, *34*, 778–786; c) M. Hernández-Molina, J. González-Platas, C. Ruiz-Pérez, F. Lloret, M. Julve, *Inorg. Chim. Acta* **1999**, *284*, 258–265; d) H. Grove, J. Sletten, M. Julve, F. Lloret, *J. Chem. Soc. Dalton Trans.* **2001**, 2487–2493; e) G. A. van Albada, O. Roubeau, P. Gamez, H. Kooijman, A. L. Spek, J. Reedijk, *Inorg. Chim. Acta* **2004**, *357*, 4522–4527; f) F. J. Barros-García, A. Bernalte-García, F. J. Higes-Rolando, F. Luna-Giles, A. M. Pizarro-Galán, E. Viñuelas-Zahínos, *Z. Anorg. Allg. Chem.* **2005**, *631*, 1898–1902; g) X.-L. Li, B.-L. Liu, Y. Song, *Inorg. Chem. Commun.* **2008**, *11*, 1100–1102; h) W. A. Alves, I. O. Matos, P. M. Takahashi, E. L. Bastos, H. Martinho, J. G. Ferreira, C. C. Silva, R. H. de Almeida Santos, A. Paduan-Filho, A. M. Da Costa Ferreira, *Eur. J. Inorg. Chem.* **2009**, 2219–2228; i) H. Liu, F. Gao, D. Niu, J. Tian, *Inorg. Chim. Acta* **2009**, *362*, 4179–4184.



- [19] a) T. Rojo, M. I. Arriortua, J. Ruiz, J. Darriet, G. Villeneuve, D. Beltran-Porter, *J. Chem. Soc. Dalton Trans.* **1987**, 285–291; b) X.-H. Bu, M. Du, Z.-L. Shang, L. Zhang, Q.-H. Zhao, R.-H. Zhang, M. Shionoya, *Eur. J. Inorg. Chem.* **2001**, 1551–1558; c) F. B. Tamboura, M. Gaye, A. S. Sall, A. H. Barry, T. Jouini, *Inorg. Chem. Commun.* **2002**, 5, 235–238; d) W. A. Alves, R. H. de Almeida Santos, A. Paduan-Filho, C. C. Becerra, A. C. Borin, A. M. Da Costa Ferreira, *Inorg. Chim. Acta* **2004**, 357, 2269–2278; e) S. Demeshko, G. Leibel, S. Dechert, F. Meyer, *Dalton Trans.* **2004**, 3782–3787; f) S.-L. Ma, X.-X. Sun, S. Gao, C.-M. Qi, H.-B. Huang, W.-X. Zhu, *Eur. J. Inorg. Chem.* **2007**, 846–851; g) E. Gungor, H. Kara, *Inorg. Chim. Acta* **2012**, 384, 137–142.
- [20] a) M. Verdaguer, *Polyhedron* **2001**, 20, 1115–1128; b) H. Oshio, M. Nakano, *Chem. Eur. J.* **2005**, 11, 5178–5185; c) D. Gatteschi, A. Cornia, M. Mannini, R. Sessoli, *Inorg. Chem.* **2009**, 48, 3408–3419; d) H. Miyasaka, M. Julve, M. Yamashita, R. Clérac, *Inorg. Chem.* **2009**, 48, 3420–3437.
- [21] a) R. Mukherjee, in: *Comprehensive Coordination Chemistry-II: From Biology to Nanotechnology*, vol. 6 (Eds.: J. A. McCleverty, T. J. Meyer), Volume Ed.: D. E. Fenton, Chapter on Copper, Elsevier, Amsterdam, **2003**, 747; b) R. Mukherjee, *Coord. Chem. Rev.* **2000**, 203, 151.
- [22] a) J. Astner, M. Weitzer, S. P. Foxon, S. Schindler, F. W. Heinemann, J. Mukherjee, R. Gupta, V. Mahadevan, R. Mukherjee, *Inorg. Chim. Acta* **2008**, 361, 279–292; b) R. Gupta, R. Mukherjee, *Polyhedron* **2000**, 19, 719–724; c) S. Mandal, F. Lloret, R. Mukherjee, *Inorg. Chim. Acta* **2009**, 362, 27–37.
- [23] I. Dvoretzky, G. H. Richter, *J. Org. Chem.* **1950**, 15, 1285–1288.
- [24] W. J. Geary, *Coord. Chem. Rev.* **1971**, 7, 81–122.
- [25] L. J. Farrugia, *WINGX*, Version 1.64, An Integrated System of Windows Programs for the Solution, Refinement and Analysis of Single-Crystal X-ray Diffraction Data; Department of Chemistry: University of Glasgow, **2003**.
- [26] *DIAMOND*, Version 2.1c, Crystal Impact GbR, Bonn, Germany, **1999**.
- [27] A. W. Addison, T. N. Rao, J. Reedijk, J. van Rijn, G. C. Verschoor, *J. Chem. Soc. Dalton Trans.* **1984**, 1349–1356 (square pyramidal geometry  $\tau = 0$ ; trigonal bipyramidal geometry  $\tau = 1$ ).
- [28] J. C. Bonner, M. E. Fischer, *Phys. Rev. A* **1964**, 135, 640–658.

Received: January 3, 2014  
Published Online: March 7, 2014